

# Mission grass bio-waste functional carbon self-single- doped for ultrahigh energy symmetrical supercapacitor

*by Rika Taslim*

---

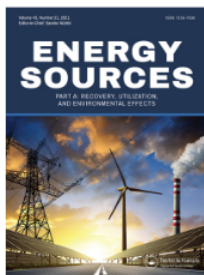
**Submission date:** 04-Aug-2023 11:47AM (UTC+0700)

**Submission ID:** 2141136460

**File name:** single\_doped\_for\_ultrahigh\_energy\_symmetrical\_supercapacitor.pdf (2.04M)

**Word count:** 7357

**Character count:** 41553



## Mission grass bio-waste functional carbon self-single-doped for ultrahigh energy symmetrical supercapacitor

Rika Taslim, Farhan Dio Pahlevi, <sup>36</sup> Muhammad Ihsan Hamdy, Apriwandi Apriwandi & Erman Taer

To cite this article: Rika Taslim, Farhan Dio Pahlevi, <sup>36</sup> Muhammad Ihsan Hamdy, Apriwandi Apriwandi & Erman Taer (2023) Mission grass bio-waste functional carbon self-single-doped for ultrahigh energy symmetrical supercapacitor, Energy Sources, Part A: Recovery, Utilization, and Environmental Effects, 45:4, 9928-9940, DOI: [10.1080/15567036.2023.2242320](https://doi.org/10.1080/15567036.2023.2242320)

To link to this article: <https://doi.org/10.1080/15567036.2023.2242320>



Published online: 01 Aug 2023.



Submit your article to this journal [↗](#)






View related articles [↗](#)



View Crossmark data [↗](#)



## Mission grass bio-waste functional carbon self-single-doped for ultrahigh energy symmetrical supercapacitor

Rika Taslim <sup>a</sup>, Farhan Dio Pahlevi<sup>a</sup>, Muhammad Ihsan Hamdy<sup>a</sup>, Apriwandi Apriwandi <sup>b</sup>, and Erman Taer <sup>b</sup>

<sup>a</sup>Department of Industrial Engineering, State Islamic University Sultan Syarif Kasim, Pekanbaru, Indonesia;

<sup>b</sup>Department of Physics, Faculty of Mathematic and Natural Sciences, University of Riau, Pekanbaru, Indonesia

### ABSTRACT

Several studies have been performed on biomass as an extraordinary natural carbon resource for functional electrode with combined pore structure, self-doping, and nanopores morphology significantly boosted supercapacitor performance. Therefore, this study utilized mission-grass bio-waste as a porous carbon source self-single-doped as electrode material capable of increasing the energy density of supercapacitor. Porous carbon was obtained through the chemical impregnation synthesis route of  $ZnCl_2$  and physical activation at temperatures 800, 850, and 900°C. The precursor materials were designed solid shape-like without adding synthetic materials. The optimized mission-grass-based porous carbon (MGPCs) illustrates the diverse pore structure, and wettability properties of the oxygen (O) internal doped. With supercapacitor symmetrical system, the MGPCs electrode showed the highest electrochemical properties at capacitive behavior as high as  $208 F g^{-1}$  in  $1 A g^{-1}$  with  $H_2SO_4$  electrolyte. Furthermore, the energy density of the electrodes was increased by  $28.31 Wh kg^{-1}$  with good electrical conductivity at internal resistance at  $0.139\Omega$ . The high electrochemical performance of the MGPCs electrodes proved that the insertion of mission grass biomass into porous carbon converted through an environmentally benign strategy obtained high-quality electrode material to boost the energy density of the supercapacitor.

### ARTICLE HISTORY

Received 22 May 2023

Revised 20 July 2023



Accepted 24 July 2023

### KEYWORDS

Porous carbon; biomass; electrode materials; symmetrical supercapacitor

### Introduction

This decade is considered the highest level of human modernization because it is marked by the development of the global economy, the extraordinary growth of the technology industry, as well as the evolution of biotechnology and cultural engineering, thereby leading to a rapid increase in the level of prosperity globally (Szocik and Braddock 2022). However, this modernization increase has some determinantal effects, such as higher pollution levels, quick consumption of nonrenewable energy sources, and demolishing ecological contamination, which decreases public health and the survival of the next generation (Deng et al. 2022). The world's major institutions have tried to apply a common frame of mind for “green growth technology” to accelerate the transfer of conventional energies to renewable green resource technologies (Guo et al. 2020). Among the numerous intensive researches on increasing renewable energy conversion, the supercapacitor is considering broadly concentrated prevalent energy storage in view of its uncommon elements (Alem et al. 2022; Ciszewski et al. 2019). These include unlimited life cycle, relatively fast charging-discharge in minute scale, extraordinary power density, system safe operation, long service life, and high component stability (González et al.

**CONTACT** Rika Taslim  [rikataslim@gmail.com](mailto:rikataslim@gmail.com)  Department of Industrial Engineering, State Islamic University Sultan Syarif Kasim, Simpang Baru, Pekanbaru 28293, Indonesia

© 2023 Taylor & Francis Group, LLC

2016; Majid et al. 2021). These advantages enable supercapacitors as prime candidates to develop the next generation of energy conversion, particularly in the practical application of electronic components, spare parts, hybrid vehicles, pulse laser components, and crane and lift auxiliary systems (Deraman et al. 2016; Iro, Subramani, and Dash 2016). However, supercapacitors are considered to still have obstacles in their practical application, especially at low energy densities lower than conventional fuel cells and batteries. The increase in energy density is heavy because it erodes their high power performance. To overcome this problem, numerous serious investigations have been committed to expanding the energy output and limit of supercapacitors without lessening their power output. The strategies used to improve the promising, effective and efficient electrochemical performance of supercapacitors' are 2D nanostructures, pore hierarchies, heteroatom doping, selecting the appropriate electrolyte with higher voltage operation, and excellent ionic conductivity (Pal et al. 2019; Wang, Zhang, and Zhang 2012). The combination of these extraordinary properties leads to high energy densities while maintaining their power densities. Furthermore, the design of the electrode material through the incorporation and transition of metal oxides, such as ruthenium, nickel, and vanadium, demonstrates stability during redox reactions in an easily accessible and abundant pore distribution (Dhara and Mahapatra 2019). Additionally, among various metal oxides,  $\text{MnO}_2$  is the leading compound that exhibits superior electrochemical behavior with important applications in many energy conversion and storage processes (Long et al. 2020). Meanwhile, electrospinning and hard, soft, and salt template methods based on polymeric materials, such as polypyrrole and polyaniline, allow electrode materials to have rich, regular 2D nanostructures, abundant hierarchical pores that lead to high material conductivity properties, excellent ion accessibility, and good flexibility (Zang et al. 2020). Zhang et al. (2017) reported that graphene-polymer-based electrodes with 3D pore features are able to compete with the battery energy output as  $28.06 \text{ Wh kg}^{-1}$  in high specific capacitance of  $1,182 \text{ F g}^{-1}$  (Zhang et al. 2017). However, the synthesis routes described are relatively complex, expensive to manufacture, corrosive, and toxic, thereby compromising their service life and hindering the goal of green and environmentally benign energy storage. Biomass is generally known as one of the abundant natural resources with extraordinary potential energy sources and conversion. Several studies suggest that the world's total land biomass is about 1.8 trillion tons each, with a potential energy production capacity of 33,000 EJ (Tursi 2019). Its conversion value is 80 times greater than the world's annual energy consumption. Interestingly, the high carbon source in biomass has tremendous potential as a base material for high-quality electrodes. Because of its controllable permeable construction, novel nanostructure potential, great physical-compound dependability, high electrical conductivity, and bountiful heteroatom doping, biomass-based actuated carbon utilizes roughly 80% of the terminal base material for electrochemical supercapacitor (Abbas et al. 2019; Saini, Chand, and Joshi 2021; Zhang et al. 2017). Moreover, biomass is cheap, bounteously accessible, practical, harmless to the ecosystem, simple combination course, and nonpoisonous destructive, consequently, it is entirely reasonable to be created as a wellspring of green terminal material for maintainable supercapacitor applications (Herou et al. 2018; Li et al. 2020). Several recent studies have reported the potential of waste biomass as electrode material, such as yellow mangosteen (Taer et al. 2023), onion skin (Gopalakrishnan and Badhulika 2021), eucalyptus wood (Atika and Dutta 2021), camellia husk (Cui et al. 2022), *Osmanthus fragrans* (Quan et al. 2018), *Laurus nobilis* (Taer et al. 2023), sakura flower (Ma et al. 2019), mangosteen (Yang et al. 2019), and *Solanum torvum* Fruit (Taer et al. 2023). The *Averrhoa bilimbi* leaves are an extraordinary features of 3D pores structured and internal doped heteroatom with impressive energy densities of  $26.54 \text{ Wh kg}^{-1}$  in a symmetrical supercapacitor system (Taer et al. 2022). Li et al. reported the potential of the eggplant as a porous carbon electrode with similar features with an increase in power density reaching  $38 \text{ Wh kg}^{-1}$  (Li et al. 2022). However, the time-consuming synthesis route and real low stability need to be optimized by intensely finding a truly promising approach. In addition, mission grass was confirmed to provide abundant



lignocellulose components with the proportion of lignin (15.6%), cellulose (40.02%), and hemicellulose (29.2%). This combination of elements makes it possible to provide unique nanopores that enhance the precursor material features.

This study utilized the ecologically harmless and efficient way to deal with getting biomass-based permeable carbon as a quality cathode material for symmetric supercapacitor applications. Biomass antecedents of mission grass were characterized in the entirety of their novel potential, while the compound impregnation blend course at high-temperature pyrolysis got permeable carbon. The material properties of the permeable carbon were controlled through various actual initiation temperatures, including 800, 850, and 900°C. The characterization of the material properties results showed that the optimized precursor had a high amorphous carbon structure, with various hierarchically connected pores, and a high purity carbon state. Furthermore, the electrochemical properties exhibit high capacitive properties of 208 F g<sup>-1</sup> in 1 A g<sup>-1</sup> with H<sub>2</sub>SO<sub>4</sub> electrolyte at an energy output of 28.31 Wh kg<sup>-1</sup> in a symmetric supercapacitor system. The proposed earth-harmless methodology expressly investigates mission-grass-based permeable carbon as a forerunner terminal hotspot for reasonable electrochemical supercapacitor.

## Methodology

### *Mission grass-based biomass porous carbon preparation (MGPCs)*

One sack of mission grass waste that grows wild in Pekanbaru, Riau Province, is collected, washed with running water, and cut into small pieces about 5 cm in size. The examples were dried in the sun for a few days and continued with electrical dried at 101°C. Consequently, the precursors were pre-carbonization by around 30 g at 250°C in a vacuum stove. The pre-carbonized samples were also crushed using a milling machine until the samples were in powder form and then sieved in 60 μm sieve. The powdered precursor was synthetically enacted in a ZnCl<sub>2</sub> arrangement with a convergence of 0.5 mmol/L utilizing a hot plate at 79–81°C and 300 rpm and dried in a broiler at 110°C for 48 hours. Then, carbon synthetically enacted was printed to stone monuments (coins) involving a water driven press with 15 stone monuments for every treatment. The example was then carbonized by pyrolysis at room temperature to a greatest temperature of 600°C in a N<sub>2</sub> vaporous gas, trailed by actual enactment at various high temperatures, for example, 800°C, 850°C, and 900°C in a CO<sub>2</sub> gas. At last, the carbon stone monument tests were neutralized utilizing refined water, dried at 110°C, and named MGPC-800, MGPC-850, and MGPC-900, as per the shifting temperatures.

### *Material characterization*

The examining the electron microscopy (SEM) and energy dispersive spectroscopy (EDS) was utilized to assess morphological construction and basic status with JEOL-JSM-6510LA instrument. The graphitization confirmation was identify with X-ray diffraction (XRD) in 10–100° degree. The N<sub>2</sub> gas adsorption-desorption strategy was utilized to evaluated the porosity properties with BET, BJH, and T-plot techniques.

### *Electrochemical measurements*

The electrochemical presentation of a permeable carbon stone monument as a supercapacitor terminal was estimated in cyclic voltammetry (CV) utilizing a CV UR Rad-Er 5841 instrument adjusted by VersaStat II Princeton Applied Exploration at a blunder pace of ± 6.0%. The voltage window goes from 0 to 1 V with examine paces of 1–10 mV s<sup>-1</sup>. The functioning cathodes are collected in a symmetric supercapacitor framework in a sandwich layer drenched in a fluid electrolyte of 1 M H<sub>2</sub>SO<sub>4</sub>. Furthermore, the electrochemical properties of the examples were likewise estimated by galvanostatic charge-discharge (GCD). Explicit capacitance, energy, and power output are assessed utilizing

conditions standard. Furthermore, the strategy for electrochemical impedance spectroscopy (EIS) was additionally done to affirm the in-depth electrochemical properties of the electrode material. EIS was performed from 0.01 Hz to 100,000 Hz, with the particular capacitance, as well as energy and, not entirely settled by standard conditions in view of a symmetrical framework.

## Results and discussions

The physical activation reaction of high-temperature CO<sub>2</sub> on the carbon chain affects the surface morphology of MGPC solids, which were reviewed in detail using scanning electron microscopy (SEM) with the images of MGPC-800, MGPC-850, and MGPC900 shown in Figure 1 at different magnifications. Micrograph of MGPC-800 showed a dominated large particle aggregates, as shown in Figure 1a. In the enlarged selection area in Figure 1b, MGPC-800 displays a large pore on the particle block wall, confirming the presence of a micron-sized pore. Furthermore, the expansion in the actual enactment temperature at 850°C exhibits a relatively dominated surface morphology by small-size carbon blocks with significant aggregate breakdown. According to Figure 1c, the size of the carbon blocks varies from 0.063 μm to 2.498 μm with etching carbon chains at high temperatures, which allows dramatic erosion of the lignocellulosic components, thereby affecting the surface structure. Significant erosion of cellulose and lignin initiates the formation of 2D nanostructures, such as tubular, fiber, and sheet (Kumar et al. 2020; Taer et al. 2020). Figure 1d displays a magnified area of

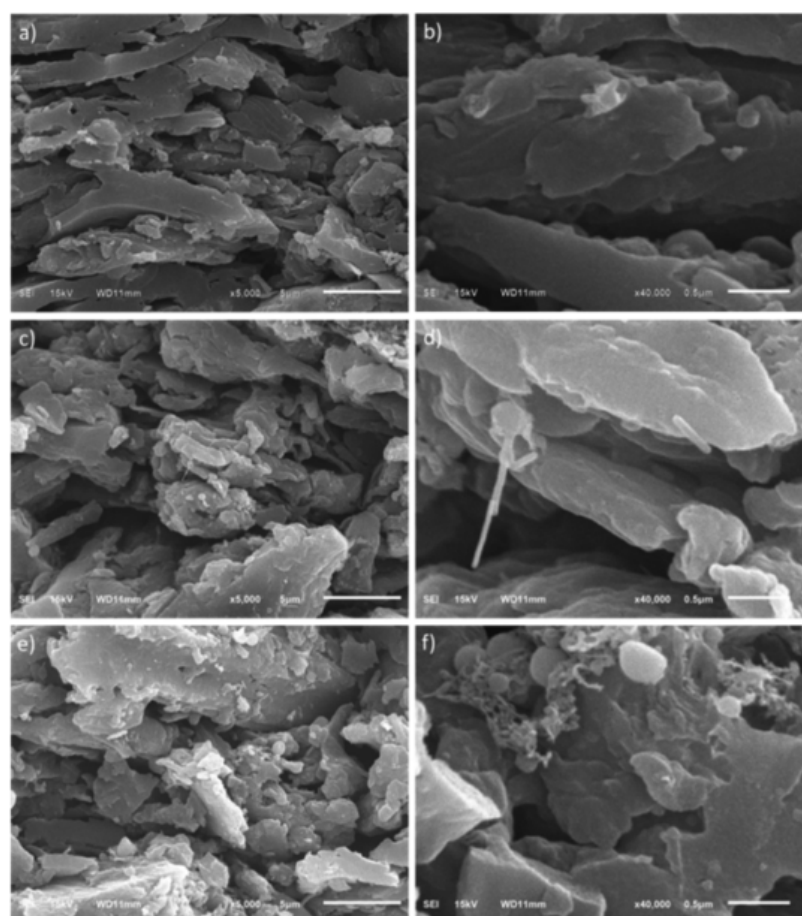


**Figure 1.** Image SEM for (a,b) MGPC-800, (c,d) MGPC-850, and (e,f) MGPC-900 in 5000× and 40,000× magnification.

the MGPC-850 SEM image confirming a morphological structure resembling a rod/tube at 30–36 nm diameter. The etching of optimal carbon chains occurs at 850°C with morphology that leads to 2D nanostructures. The continuous erosion of the particle aggregate at high temperatures up to 900°C allows the precursor-based material to undergo significant morphological changes, as shown in Figure 1e. The MGPC-900 displays relatively large pores in the macropores range with aggregates ranging from 0.238  $\mu\text{m}$  to 2.276  $\mu\text{m}$  and relatively larger than MGPC-850. Furthermore, in the selected area selection, the MGPC-900 displays pores of various mesoporous scales interconnected in 3D. These pore characteristics contribute significantly to ion accessibility and barrier-free charge transfer on the electrode material to maintain high power density performance in supercapacitor energy storage components (Hao et al. 2017). The degree of crystallinity and phase change that occurred in the porous carbon of MGPCs was assessed using an X-ray diffraction (XRD) pattern, as shown in Figure 2. It showed two significant broad peaks at  $2\theta$  approximately 21.53°, 24.15°, and 24.76° indexed to the scattering plane (002) and 42.71°, 44.91°, and 45.44° which are correlated to the scattering plane (100) of MGPC-800, MGPC-850, and MGPC-900, respectively. It further characterizes the amorphous-turbostratic carbon structure rich in pores and attenuated crystallinity (JCPDS No. 41–1487) (Peng et al. 2013; Sodtipinta et al. 2017), which proves that the sample has a confirmed pore structure. Expansion in the actual enactment temperature at MGPC800 to MGPC-850 displays a shift of the indexed width peak (002) toward a smaller one, thereby confirming the abundant increase in the growth of narrow pores. Additionally, the broad peak in the scattering plane (100) shifted to a greater extent from 42.487° to 45.710°, allowing MGPC-850 to have confirmed mesopores on the precursor surface. The combined features of microporous and mesoporous growth in the based material contribute to the electrode's high capacitive properties and low internal resistance. This analysis is further justified through the analysis of electrochemical properties using CV and GCD techniques. However, an expansion in the actual enactment temperature up to 900°C displays a different pattern and leads to the opposite feature, thereby confirming a good reduction in pore development. This is because excessive carbon chain etching at 900°C harmed the pore system construction of the

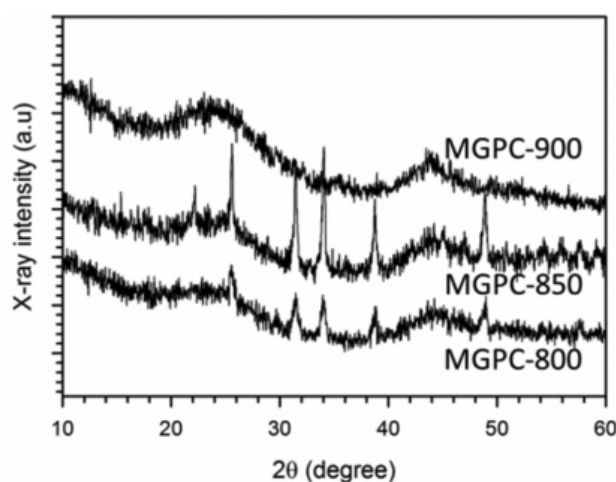


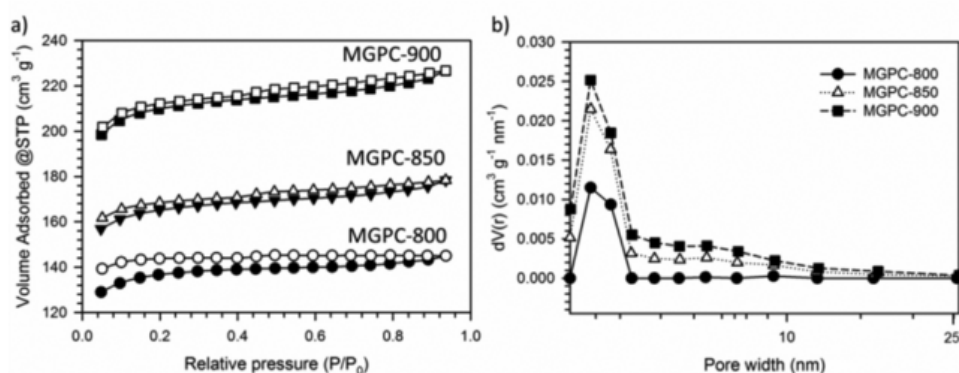
Figure 2. XRD pattern of MGPCs.

Table 1. Porosity properties and elemental status of MGPCs.

Precursor	$S_T$ ( $\text{m}^2 \text{g}^{-1}$ )	$S_{\text{micro}}$ ( $\text{m}^2 \text{g}^{-1}$ )	$S_{\text{meso}}$ ( $\text{m}^2 \text{g}^{-1}$ )	$V_{\text{tot}}$ ( $\text{cm}^3 \text{g}^{-1}$ )	$V_{\text{micro}}$ ( $\text{cm}^3 \text{g}^{-1}$ )	$V_{\text{meso}}$ ( $\text{cm}^3 \text{g}^{-1}$ )	$D_{\text{ave}}$ (nm)	C (%)	O (%)	Zn (%)	Si (%)
MGPC-800	416.892	400.299	16.593	0.225	0.206	0.019	1.078	93.73	4.51	1.34	0.42
MGPC-850	503.551	476.252	27.299	0.277	0.245	0.032	1.099	93.89	4.02	1.55	0.55
MGPC-900	639.414	605.048	34.366	0.352	0.312	0.040	1.099	93.13	6.02	0.00	0.84



antecedent. The ratio of basic parts present in MGPCs is uncovered through energy dispersive spectroscopy (EDS) estimations, and it summarized in Table 1. Evaporation of water content, volatiles, polysaccharides, and hemicelluloses, as well as degradation of other organic components due to carbonization in inert gases, initiates the production of high carbon fixed. Furthermore, the high physical activation temperature followed by carbon chain removal significantly reduced the lignocellulosic content leading to the strengthening of the porous carbon skeleton. Table 1 show that the main constituent elements of all samples were dominated by high carbon at 93.73%, 93.89%, and 93.13% for MGPC-800, MGPC-850, and MGPC-900, respectively. This high carbon content permits the terminal material to deliver high electrical conductivity properties followed by a low comparable series opposition, improving the supercapacitor's extraordinary execution. Alternately, oxygen possesses the second most elevated component in the scope of 4.02% to 6.02% in light of the fact that the exorbitant carving of carbon chains by  $\text{CO}_2$  permits the antecedent to create oxidation results that tight spot to inorganic parts. The high oxygen content has a positive side for the electrode material, especially in their contribution to the improvement of wettability, maintained conductivity, self-doping of heteroatoms, and the pseudo-capacitance effect on supercapacitor (Abbas et al. 2019; Zheng et al. 2021). Due to incomplete evaporation of the remaining pyrolysis production, Silicon and zinc are also found in small amounts in MGPC. The porosity conduct of the MGPCs acquired from high-temperature pyrolysis contrast in regards to the  $\text{N}_2$  sorption isotherm and pore size conveyance, as displayed in Figure 3a–b and summed up in Table 1. The  $\text{N}_2$  isotherm adsorption-desorption profiles of MGPCs show a noticeable mix of elements of the kind sort I and type IV bends, as displayed in Figure 3a. High  $\text{N}_2$  absorption in the region of very low relative pressure characterizes strong I-type features, indicating that more than 90% of micropores dominate MGPCs. This component is likewise affirmed in Table 1, which shows that the typical pore width of MGPCs is around 1 nm. Micropores are bountiful on the 1 nm pore size, subsequently causing an extreme expansion in the particle pool at the electrolyte/terminal connection point, starting the advancement of strangely high unambiguous capacitance. This assumption is analyzed more deeply in CV and GCD measurements. At the same time, the hysteresis loops displayed over a greater relative pressure region confirm the presence of type-IV, closely related to defined mesoporosity. This feature is useful to increase the accessibility of ionic charges on absorption surfaces for the electrolyte ions to move in all directions, thereby initiating an increase in fast currents and high-power capabilities. However, the hysterical loop on MGPC-800 is imperfect (not closed) and reflects the creation of imperfect mesopores with the assumption that the pore shape resembles a “bottleneck” with a narrow pore surface and relatively large space on the inside. The defect of the mesoporous structure can be corrected by increasing the pyrolysis temperature. The higher porosity temperature in MGPC-850 and MGPC-900 indicates an increase in the mesopores structure, which is illustrated by their better hysteresis loop compared to MGPC-850. Figure 2b shows that the expanded pyrolysis temperature expanded the pore size



44  
Figure 3. (a) Nitrogen adsorption-desorption profiles and (b) the pore size distribution (PSD) of MGPCs.



circulation on the mesoporous scale with a typical size of 3.62 nm. This additionally builds the mesoporous volume from  $0.019 \text{ cm}^3 \text{ g}^{-1}$  to  $0.040 \text{ cm}^3 \text{ g}^{-1}$ , as displayed in Table 1. The expansion in pyrolysis temperature can essentially raise the development of the particular surface area of MGPCs from 800 to  $900^\circ\text{C}$ , with a fast ascent in the particular surface region coming to  $\pm 53\%$  of  $639.414 \text{ m}^2 \text{ g}^{-1}$ . In addition, their micropore predominance is likewise advanced to 94.6% with clear-cut mesopores, which all the while act as the principal key to helping the high electrochemical presentation of cathode materials. These incorporate expanding the particular capacitance and energy output without un-

mining their power output. The electrochemical performance of the MGPCs electrode was first traced through the cyclic voltammetry (CV) strategy in a symmetrical configuration at  $\text{M H}_2\text{SO}_4$  liquid electrolyte. The CV profiles at  $1 \text{ mV s}^{-1}$  of the MGPC-800, MGPC850, and MGPC-900 illustrate a distorted/non-ideal rectangular shape (Figure 4a), thereby revealing normal electrical double-layer properties (Climent

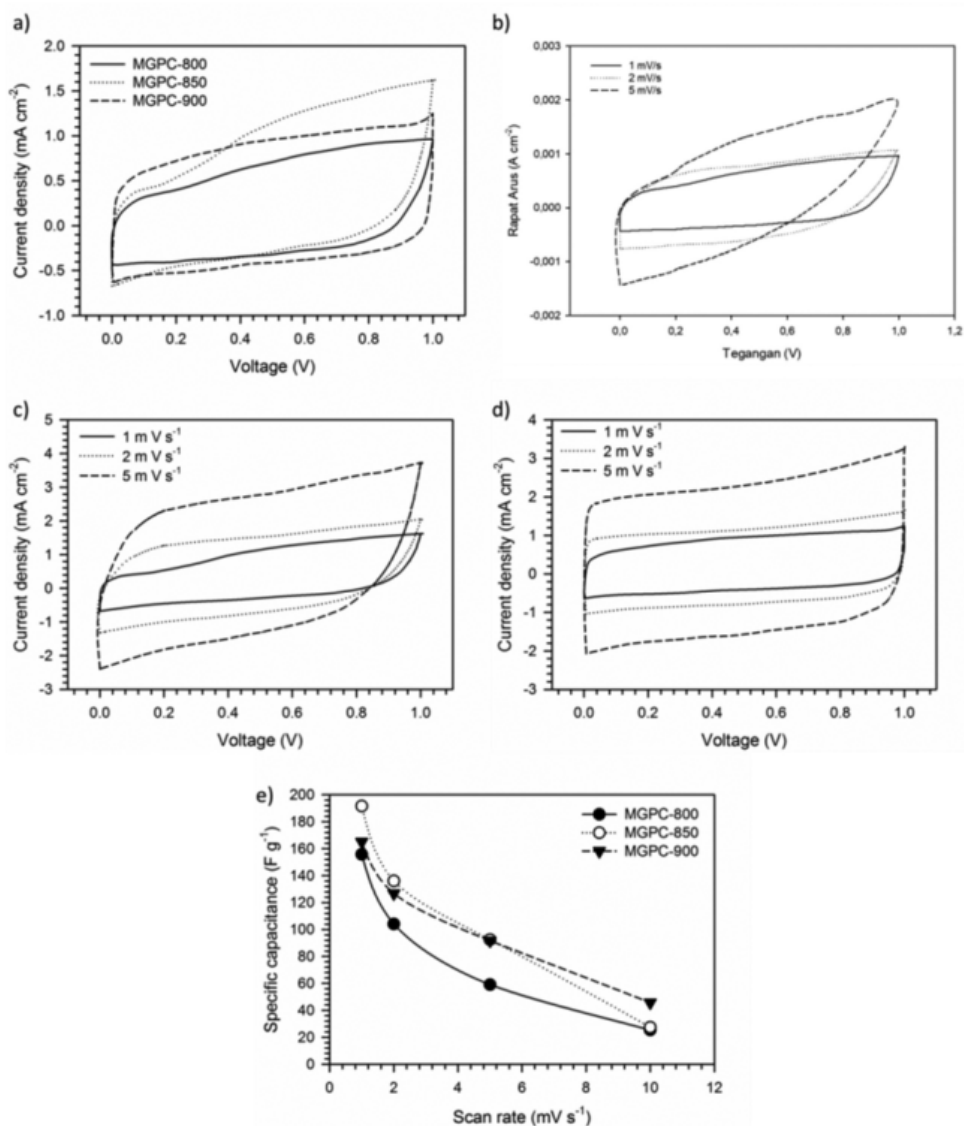


Figure 4. CV profile of MGPCs samples (a) at scan rate  $1 \text{ mV s}^{-1}$ , (b) MGPC-800 at scan rate  $1\text{--}5 \text{ mV s}^{-1}$ , (c) MGPC-850 at scan rate  $1\text{--}5 \text{ mV s}^{-1}$ , (d) MGPC-900 at scan rate  $1\text{--}5 \text{ mV s}^{-1}$ , and (e) Specific capacitance vs. Scan rate.

and Feliu 2018; Taer et al. 2018). The MGPC-800 electrode displays a relatively small CV profile, which characterizes its low capacitive properties. In the low voltage range  $V < 0.1$  V, the current density increases suddenly, confirming that the ionic charge is simultaneously transmigrated to the micropores on the electrode surface. Furthermore, their CV profile tends to slope at higher potential ranges, confirming the relatively low ionic charge transfer in the large pores with a low capacitance of  $155 \text{ F g}^{-1}$ . On the other hand, the MGPC-850 electrode displayed the largest charge-discharge loop hysteresis, confirming the highest electrochemical properties. At a potential  $< 0.1$ , the current density increased significantly, indicating that the micropores-rich MGPC-850 material filled with electrolytic ions formed the first electrical double layer. The unexpected expansion in current thickness that frames a “camel bump” in the voltage range  $0.20 < V < 0.50$  shows a useful commitment of oxygen as a self-doping heteroatom that initiates the faradaic reaction in the electrode material (Meng et al. 2020), which presents a pseudo-capacitance effect on the electrochemical properties of MGPC-850. Interestingly, in the voltage range  $V > 0.6$  V, the current density continued to increase drastically until  $V = 1.0$  V, indicating that the mesoporous MGPC-850 is optimally accessed by the electrolytic ion charge adding to the abundant electrochemical double layer capacitor. The elite presentation mix of the MGPC-850 cathode shows an expanded capacitance worth of  $191 \text{ F g}^{-1}$ . This demonstrates that blending activated carbon derived organic precursor as cathode sources by expanding the actual actuation temperature of  $\text{CO}_2$  builds the particular capacitance of the supercapacitor, particularly in the symmetrical arrangement framework. However, the increased physical activation temperature on the MGPC-900 did not display the same characteristic. The CV profile displayed by the MGPC-900 electrode is relatively similar to the MGPC-800, indicating that their capacitive properties are the same. The reduction of amorphous and carbon content of MGPC-900, which XRD and EDS analyzed, had a major impact on the reduction of the electro-analytical behavior of MGPC-900. The capacitance feature obtained in the symmetric cell MGPC-900 is about  $165 \text{ F g}^{-1}$ . The electrochemical features of MGPCs were confirmed through scan rates at  $1\text{--}5 \text{ mV s}^{-1}$ , as illustrated in Figure 4b–d. The CV shape generally performed an increasingly ideal rectangular form confirming the potential for MGPCs electrodes to have normal electrical multi-layer (EDLC) behavior based on activated carbon sources. Moreover, their cyclical performance is also reviewed in terms of capacitances feature in high scan rate, as shown in Figure 3e. The capacitance behavior of the MGPCs precursor degraded drastically at a scan rate of  $10 \text{ mV s}^{-1}$  because the carbon material has a low meso-macroporosity, therefore, the ionic charge is not optimally induced at electrolyte/terminal connection point (Y. Zhang et al. 2017). The electrochemical features of MGPCs was identify through a galvanostatic charge-discharge (GCD) which represents the detailed behavior of specific capacitive properties, electrode resistance, energy output, and power output in a symmetric cell system. The GCD profile for the terminals of MGPCs submerged at  $1 \text{ A g}^{-1}$  in  $\text{H}_2\text{SO}_4$  electrolyte is displayed in Figure 5a. In general, all electrodes in a symmetrical cell system displayed disturbed isosceles triangle curves, thereby confirming their

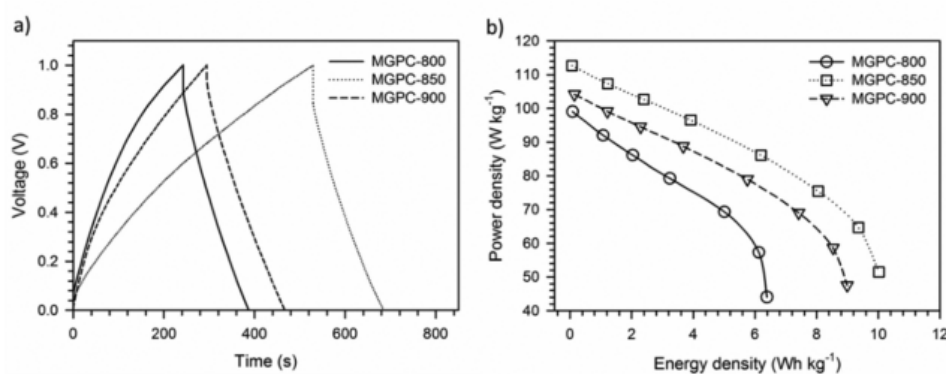
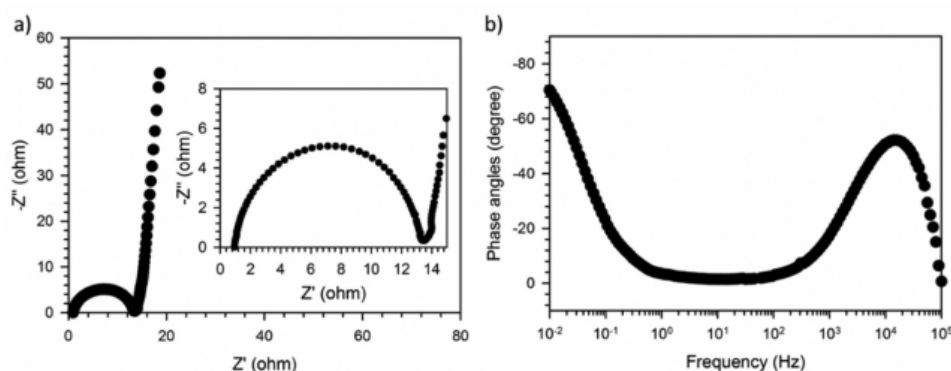


Figure 5. (a) GCD profile of MGPCs samples in  $1 \text{ M H}_2\text{SO}_4$ , and (b) Ragone plot of MGPC samples in  $1 \text{ M H}_2\text{SO}_4$ .

normal potential in the electrical layer (EDLC) type. Furthermore, their relatively long charging time compared to the discharging time indicates ion degradation in the charge transfer process. As indicated by primer investigations, the wettability of the oxygen utilitarian gathering starts the faradaic response (Luo et al. 2021). This prompts an expansion in the pseudo-capacitance property, as affirmed in the CV shape. Coulombic productivity is gotten from the information on the distinction between the charging and releasing time of the GCD ( $\eta = [t_d/t_c] \times 100\%$ ). Coulombic proficiency was found in the scope of 50–70% in MGPCs pseudocapacitance was additionally viewed because of particle corruption from doped heteroatoms, particularly self-oxygen doped. Besides, the somewhat prevailing dispersion of micropores additionally influences their proficiency. Additionally, the voltage drop, commonly known as the IR drop, is determined from the GCD profile, thereby revealing the electrode resistances of the material electrodes of 0.099, 0.154, and 0.059  $\Omega$  for MGPC-800, MGPC-850, and MGPC-900, respectively. In more detail, the relatively higher IR-drop on MGPC-800 is indicated by the effect of pore growth in the material. The rich micropores apparently inhibit the charge transport pathway during ion insertion-deinsertion at the electrolyte/terminal connection point. The time required to perform one charge and discharge cycle reflect the specific capacitance of the electrical material. According to the standard equation, the specific capacitance obtained from the MGPC-800, MGPC-850, and MGPC-900 electrodes were 166, 208, and 180  $F g^{-1}$ , respectively. Mission grass-based porous carbon synthesis routes involving chemical impregnation and physical activation of 800°C high-temperature  $CO_2$  significantly improved the high performance of supercapacitor cells in two electrode configurations of 166  $F g^{-1}$  with their relatively low cell resistance of 0.099  $\Omega$ . This is because the chosen strategy resulted in the obtained carbon material properties with high potential in porosity, surface morphology, clear elemental status, and high electrical conductivity (Selvaraj et al. 2021). Furthermore, increasing the physical activation temperature to 850°C drastically raised the capacitance feature of 208  $F g^{-1}$ , indicating that the porosity optimization and abundant active channels can accommodate the high ion migration markedly, thereby improving their electrochemical performance (Wang et al. 2021). MGPC-850 has the best amorphous properties with the highest predicted specific surface area, enabling them to form an enriched electrical double layer, thereby enhancing their capacitive properties. The presence of the pseudo-capacitance impact of practical oxygen adds to the superior exhibition of the terminal material. Notwithstanding, expanding the actual enactment temperature to 900°C prompted a reduction in capacitive properties by 180  $F g^{-1}$  because of the deformity of the pore structure in the MGPC-900 carbon material. The reduced amorphous and empirical surface area affected their capacitive behavior (Deraman et al. 2015). Meanwhile, the energy and power outputs performances of the MGPCs electrodes were possessed through the Ragone plot, as illustrated at Figure 5b. The energy output obtained from the MGPC-800, MGPC-850, and MGPC-900 are 22.64, 28.31, and 24.58  $Wh kg^{-1}$ , at optimum power output of 73.83, 65.47, and 60.62  $W kg^{-1}$ . This value is relatively similar to preliminary studies that have been reported with activated carbon sources biomass-based, such as bacterial cellulose (Hao et al. 2017) and European wood (Jain et al. 2021). The highest electrochemical performance on the MGPC-850 electrode was reviewed in detail through impedance spectroscopy on an  $H_2SO_4$  electrolyte with a measurement frequency from 0.01 Hz to 100,000 Hz. The Nyquist plot of the MGPC-850 electrodes, shows in Figure 6a, shows that their curve consists of several sections. Firstly, the high frequency semicircular curvature confirms the ions' rapid migration at electrolyte/terminal connection point, which affects the inserti-deinserti in the electrode material (Lämmel et al. 2013). Secondly, the first  $Z'$  axis intercept characterizes the selected electrolyte resistance of 0.038 $\Omega$ , while the second  $Z'$  intercept represents the equivalent series resistance (ESR) reflecting the MGPC850 electrode's electronic resistance of 0.139  $\Omega$ . This low resistance is due to the contribution of high porosity followed by the wettability properties of the optimized oxygen internal doped in the MGPC-850 material (Yadav et al. 2020). The Warburg curve found at intermediate frequencies indicates fluctuating ion insertions into the framework structure carbon, as shown in insert Figure 5a. At low frequencies, the vertical line pattern clearly reflects the hallmarks of an ideal electrical dual layer response, which is also in agreement with the analysis revealed in the CV and GCD measurements. Figure 6b shows the Bode phase plot in the low to a high-frequency





**Figure 6.** (a) the Nyquist plot of the MGPC-850, and (b) the Bode phase plot of the MGPC-850.

range of the MGPC-850 electrode. At low frequencies, the value of the phase angle is about  $-78^\circ$ , which affirms the capacitive way of behaving of the typical permeable carbon-based electrical twofold layer with low opposition and high charge move (Atika and Dutta 2021). Furthermore, the knee recurrence at the staging point of  $-45^\circ$  decides the unwinding season of the anode material, which is firmly connected with the release and charge time proficiency at the cathode/electrolyte interface. The unwinding time consistent of the MGPC-850 viewed as through the  $1/f_0$  condition is 25.12 ms, which shows great terminal materials for down to earth applications in electrochemical supercapacitor.

## Conclusions

In conclusion, this research effectively applied an eco-harmless and efficient methodology as a top-notch terminal material for the change of mission-grass biomass into permeable carbon for sustainable power stockpiling gadgets. The pore morphological highlights, amorphism, wettability, and natural status were completely controlled through the actual enactment temperatures of 800, 850, and 900°C. Moreover, an expansion in the actual enactment temperature fundamentally influences the progressions in their pore morphology, prompting the development of progressively associated 3D pores. In the improved permeable carbon, the natural condition of high carbon is 93.89%, with the wettability properties contributed by the oxygen practical gathering. The nebulosness was essentially affirmed in the symmetrical-terminal arrangement framework to acquire explicit capacitances of 166, 208, and 180 F g<sup>-1</sup> for MGPC-800, MGPC-850, and MGPC-900 cathodes, separately. The most noteworthy energy output of 28.31 Wh kg<sup>-1</sup> was found at the MGPC-850 in a H<sub>2</sub>SO<sub>4</sub> fluid electrolyte at 1 A g<sup>-1</sup>. Consequently, the proposed ecologically harmless methodology expressly investigates mission-grass-based activated carbon as a electrode sources for supportable electrochemical supercapacitor.

26

## Disclosure statement

No potential conflict of interest was reported by the author(s)

## Funding

The work was supported by the collaborative grants between universities, State Islamic University of Sultan Syarif Kasim Riau 2022 [873/Un.04/L. 1/TL.01/03/2022].



## Notes on contributors

**Rika Taslim** is a lecturer at the Department of Industrial Engineering, Faculty of Science and Technology, State Islamic University of Sultan Syarif Kasim, Pekanbaru, Indonesia. Apart from being a lecturer, she is also active in research. Her research focuses on the technology of electrochemical energy storage.

**Farhan Dio Pahlevi** is a under graduate student from the Department of Industrial Engineering, Faculty of Science and Technology, State Islamic University of Sultan Syarif Kasim, Pekanbaru, Indonesia.

**Muhammad Ihsan Hamdy** is a lecturer at the Department of Industrial Engineering, Faculty of Science and Technology, State Islamic University of Sultan Syarif Kasim, Pekanbaru, Indonesia.

**Apriwandi Apriwandi** is a master's degree student from the University of Riau, Indonesia. In addition, he is active as a researcher assistant at the Material Physics and Nanotechnology Laboratory, Faculty of Mathematics and Natural Sciences, University of Riau, Indonesia.

**Erman Taer** is a lecturer and professor in the Department of Physics, Faculty of Mathematics and Natural Sciences, University of Riau, Indonesia. In addition, he also serves as coordinator of the Material Physics and Nanotechnology Laboratory at the University of Riau. Apart from being a lecturer, he is also active in research. His research focuses on the technology of electrochemical energy storage, especially supercapacitor.

## ORCID

Rika Taslim  <http://orcid.org/0000-0003-1946-1299>

Apriwandi Apriwandi  <http://orcid.org/0000-0003-3560-5571>

Erman Taer  <http://orcid.org/0000-0003-4463-8252>

## References

1. Abbas, Q., R. Raza, I. Shabbir, and A. G. Olabi. 2019. Heteroatom doped high porosity carbon nanomaterials as electrodes for energy storage in electrochemical capacitors: A review. *Journal of Science: Advanced Materials & Devices* 4 (3):341–52. doi:10.1016/j.jsamd.2019.07.007.
2. Alem, A., T. Kalogiannis, J. Van Mierlo, and M. Bercibar. 2022. A comprehensive review of stationary energy storage devices for large scale renewable energy sources grid integration. *Renewable and Sustainable Energy Reviews* 159:11221. doi:10.1016/j.rser.2022.112213.
3. Atika, and R. K. Dutta. 2021. Oxygen-rich porous activated carbon from eucalyptus wood as an efficient supercapacitor electrode. *Energy Technology* 9 (9):1–12. doi:10.1002/ente.202100463.
4. Ciszewski, M., A. Koszorek, T. Radko, P. Szatkowski, and D. Janas. 2019. Review of the selected carbon-based materials for symmetric supercapacitor application. *Journal of Electronic Materials* 48 (2):717–44. doi:10.1007/s11664-018-35811-7.
5. Climent, V., and J. M. Gu. 2018. Cyclic voltammetry. In *Encyclopedia of interfacial chemistry: Surface science and electrochemistry*, 48–74. doi: 10.1016/B978-0-12-409547-2.10764-4.
6. Cui, J., Z. X. Zhang, H. Quan, Y. Hu, S. Wang, and D. Chen. 2022. Effect of various ammonium as activating additive on the capacitance performance of hierarchical porous carbon derived from camellia husk. *Journal of Energy Storage* 51 (July):104347. doi:10.1016/j.est.2022.104347.
7. De H., Y. Tu, H. Wang, Z. Wang, Y. Li, L. Chai, W. Zhang, and Z. Lin. 2022. Eco-environment & health environmental behavior, human health effect, and pollution control of heavy metal (loid)s toward full life cycle processes. *Environment & Health* 1 (4):229–43. doi:10.1016/j.eehl.2022.11.003.
8. Deraman, M., R. Daik, S. Soltaninejad, N. S. M. Nor, Awitdrus, R. Farma, N. F. Mamat, N. H. Basri, and M. A. R. Othman. 2015. A new empirical equation for estimating specific surface area of supercapacitor carbon electrode from X-ray diffraction. *Advanced Materials Research* 1108:1–7. doi:10.4028/www.scientific.net/AMR.1108.1.
9. Deraman, M., N. S. M. Nor, Erman Taer, B. Yatim, Awitdrus, R. Farma, N. H. Basri, M. A. R. Othman, R. Omar, M. R. M. Jasni, et al. 2016. Review of energy and power of supercapacitor using carbon electrodes from fibers of oil palm fruit bunches. *Materials Science Forum* 846:451–504. doi:10.4028/www.scientific.net/MSF.846.497.
10. Dhara, K., and D. R. Mahapatra. 2019. Recent advances in electrochemical nonenzymatic hydrogen peroxide sensors based on nanomaterials: A review. *Journal of Materials Science* 54 (19):12319–57. doi:10.1007/s10853-019-03750-y.
11. González, A., E. Goikolea, J. A. Barrera, and R. Mysyk. 2016. Review on supercapacitors: Technologies and materials. *Renewable and Sustainable Energy Reviews* 58:1189–206. doi:10.1016/j.rser.2015.12.249.
12. Gopalakrishnan, A., and S. Badhulika. 2021. From onion skin waste to multi-heteroatom self-doped highly wrinkled porous carbon nanosheets for high-performance supercapacitor device. *Journal of Energy Storage* 38:102533. doi:10.1016/j.est.2021.102533.

- Guo, M., J. Nowakowska-Grunt, V. Gorbanyov, and M. Egorova. 2020. Green technology and sustainable development: Assessment and green growth frameworks. *Sustainability* 12 (16):6571–84. doi:10.3390/su12166571.
- Hao, X., J. Wang, B. Ding, Y. Wang, Z. Chang, H. Dou, and X. Zhang. 2017. Bacterial-cellulose-derived interconnected meso-microporous carbon nanofiber networks as binder-free electrodes for high-performance supercapacitors. *Journal of Power Sources* 352:34–41. doi:10.1016/j.jpowsour.2017.03.088.
- Herou, S., P. Schlee, A. B. Jorge, and M. Titirici. 2018. Biomass-derived electrodes for flexible supercapacitors. *Current Opinion in Green and Sustainable Chemistry* 9:18–24. doi:10.1016/j.cogsc.2017.10.005.
- Iro, Z. S., C. Subramani, and S. S. Dash. 2016. A brief review on electrode materials for supercapacitor. *International Journal of Electrochemical Science* 11 (12):10628–43. doi:10.20964/2016.12.50.
- Jain, A., M. Ghosh, M. Krajewski, S. Kurungot, and M. Michalska. 2021. Biomass-derived activated carbon material from native European deciduous trees as an inexpensive and sustainable energy material for supercapacitor application. *Journal of Energy Storage* 34 (December 2020):102178. doi:10.1016/j.est.2020.102178.
- Kumar, T. R., R. A. Senthil, Z. Pan, J. Pan, and Y. Sun. 2020. A tubular-like porous carbon derived from waste American poplar fruit as advanced electrode material for high-performance supercapacitor. *Journal of Energy Storage* 2 (September):101903. doi:10.1016/j.est.2020.101903.
- Lämmel, C., M. Schneider, M. Weiser, and A. Michaelis. 2013. Investigations of electrochemical double layer capacitor (EDLC) materials - A comparison of test methods. *Materialwissenschaft Und Werkstofftechnik* 44 (7):641–49. doi:10.1002/mawe.201300122.
- Li, W., C. Chen, H. Wang, P. Li, X. Jiang, J. Yang, and J. Liu. 2022. Hierarchical porous carbon induced by inherent structure of eggplant as sustainable electrode material for high performance supercapacitor. *Journal of Materials Research and Technology* 17:1540–52. doi:10.1016/j.jmrt.2022.01.056.
- Li, Z., D. Guo, Y. Liu, H. Wang, and L. Wang. 2020. Recent advances and challenges in biomass-derived porous carbon nanomaterials for supercapacitors. *Chemical Engineering Journal* 397 (October 2019):125418. doi:10.1016/j.cej.2020.125418.
- Long, X., L. Tian, J. Wang, L. Zhang, Y. Chen, Emin, X. Wang, W. Xie, D. Liu, Y. Fu, et al. 2020. Interconnected  $\delta$ -MnO<sub>2</sub> nanosheets anchored on activated carbon cloth as flexible electrode for high-performance aqueous asymmetric supercapacitors. *Journal of Electroanalytical Chemistry* 877:114656. doi:10.1016/j.jelechem.2020.114656.
- Luo, L., L. Luo, J. Deng, T. Chen, G. Du, M. Fan, and W. Zhao. 2021. High performance supercapacitor electrodes based on B/N Co-doped biomass porous carbon materials by KOH activation and hydrothermal treatment. *International Journal of Hydrogen Energy* 46 (63):31927–37. doi:10.1016/j.ijhydene.2021.06.211.
- Ma, F., S. Ding, H. Ren, and Y. Liu. 2019. Sakura-based activated carbon preparation and its performance in supercapacitor applications. *RSC Advances* 9 (5):2474–83. doi:10.1039/c8ra09685f.
- Majid, S., A. S. G. Ali, W. Q. Cao, R. Reza, and Q. Ge. 2021. Biomass-derived porous carbons as supercapacitor electrode: A review. *New Carbon Materials* 37 (3):546–72. doi:10.1016/S1872-5805(21)60038-0.
- Meng, S., Z. Mo, Z. Li, R. Guo, and N. Liu. 2020. Oxygen-rich porous carbons derived from alfalfa flowers for high performance supercapacitors. *Materials Chemistry and Physics* 246 (February):122830. doi:10.1016/j.matchemphys.2020.122830.
- Pal, B., S. Yang, S. Ramesh, V. Thangadurai, and R. Jose. 2019. Electrolyte selection for supercapacitive devices: A critical review. *Nanoscale Advances* 1 (10):3807–35. doi:10.1039/c9na00374a.
- Peng, C., X. B. Yan, R. T. Wang, J. W. Lang, Y. J. Ou, and Q. J. Xue. 2013. Promising activated carbons derived from waste tea-leaves and their application in high performance supercapacitors electrodes. *Electrochimica Acta* 87 (1):401–08. doi:10.1016/j.electacta.2012.09.082.
- Quan, H., X. Fan, W. Wang, W. Gao, Y. Dong, and D. Chen. 2018. Hierarchically porous carbon derived from biomass: Effect of mesopore and heteroatom-doping on electrochemical performance. *Applied Surface Science* 460:8–16. doi:10.1016/j.apsusc.2018.01.202.
- Saini, S., P. Chand, and A. Joshi. 2021. Biomass derived carbon for supercapacitor applications: Review. *Journal of Energy Storage* 39 (April):102646. doi:10.1016/j.est.2021.102646.
- Selvaraj, A. R., A. Muthusamy, I.-H. Cho, H. J. Kim, K. Senthil, and K. Prabakar. 2021. Ultrahigh surface area biomass derived 3D hierarchical porous carbon nanosheet electrodes for high energy density supercapacitors. *Carbon* 174:463–74. doi:10.1016/j.carbon.2020.12.052.
- Songpinta, J., C. Ieosakulrat, N. Poonyayant, P. Kidkhunthod, N. Chanlek, T. Amornsakchai, and P. Pakawatpanurut. 2017. Interconnected open-channel carbon nanosheets derived from pineapple leaf fiber as a sustainable active material for supercapacitors. *Industrial Crops and Products* 104:13–20. doi:10.1016/j.indcrop.2017.04.015.
- Szocik, K., and M. Braddock. 2022. Bioethical issues in human modification for protection against the effects of space radiation. *Space Policy* 62:101505. doi:10.1016/j.spacepol.2022.101505.
- Taer, E., A. Afrianda, R. Taslim, M. Krisman, A. Agustino, A. Apriwandi, and U. Malik. 2018. The physical and electrochemical properties of activated carbon electrode made from Terminalia Catappa leaf (TCL) for supercapacitor cell application. *Journal of Physics Conference Series* 1120 (1):012007. doi:10.1088/1742-6596/1120/1/012007.

- Taer, E., A. Apriwandi, S. Chow, and R. Taslim. 2023. Integrated pyrolysis approach of self-O-doped hierarchical porous carbon from yellow mangosteen fruit for excellent solid-state supercapacitor volumetric performance. *Diamond & Related Materials* 135:109866. doi:10.1016/j.diamond.2023.109866.
- Taer, E., A. Apriwandi, N. Nursyafni, and R. Taslim. 2022. Averrhoa bilimbi leaves-derived oxygen doped 3D-linked hierarchical porous carbon as high-quality electrode material for symmetric supercapacitor. *Journal of Energy Storage* 52:104911. doi:10.1016/j.est.2022.104911.
- Taer, E., Apriwandi, Windasari, R. Taslim, and M. Deraman. 2023. Novel laurel aromatic evergreen biomass derived hierarchical porous carbon nanosheet as sustainable electrode for high performance symmetric supercapacitor. *Journal of Energy Storage* 67:107567. doi:10.1016/j.est.2023.107567.
- Taer, E., N. Nursyafni, A. Apriwandi, and R. Taslim. 2023. Novel Solanum torvum fruit biomass-derived hierarchical porous carbon nanosphere as excellent electrode material for enhanced symmetric supercapacitor performance. *JOM*. doi:10.1007/s11837-023-05801-x.
- Taer, E., N. Yanti, W. S. Mustika, A. Apriwandi, R. Taslim, and A. Agustino. 2020. Porous activated carbon monolith with nanosheet/nanofiber structure derived from the green stem of cassava for supercapacitor application. *International Journal of Energy Research* 44 (13):1–14. doi:10.1002/er.5639.
- Tursi, A. 2019. A review on biomass: Importance, chemistry, classification, and conversion. *Biofuel Research Journal* 6 (2):962–79. doi:10.18331/BRJ2019.6.2.3.
- Wang, H., H. Niu, H. Wang, W. Wang, X. Jin, H. Wang, H. Zhou, and T. Lin. 2021. Micro-meso porous structured carbon nanofibers with ultra-high surface area and large supercapacitor electrode capacitance. *Journal of Power Sources* 482:228986. doi:10.1016/j.jpowsour.2020.228986.
- Wang, G., L. Zhang, and J. Zhang. 2012. A review of electrode materials for electrochemical supercapacitors. *Chemical Society Reviews* 41 (2):797–828. doi:10.1039/c1cs15060j.
- Yadav, N., Ritu, Promila, and S. A. Hashmi. 2020. Hierarchical porous carbon derived from eucalyptus-bark as a sustainable electrode for high-performance solid-state supercapacitors. *Sustainable Energy & Fuels* 4 (4):1730–46. doi:10.1039/C9SE00812H.
- Yang, V., R. A. Senthil, J. Pan, A. Khan, S. Osman, L. Wang, W. Jiang, and Y. Chen. 2019. Highly ordered hierarchical porous carbon derived from biomass waste mangosteen peel as superior cathode material for high performance supercapacitor. *Journal of Electroanalytical Chemistry* 19:113616. doi:10.1016/j.jelechem.2019.113616.
- Zang, S., J. Jiang, Y. An, Z. Li, H. Guo, Y. Sun, H. Dou, and X. Zhang. 2020. A novel porous organic polymer-derived hierarchical carbon for supercapacitors with ultrahigh energy density and durability. *Journal of Electroanalytical Chemistry* 876:114723. doi:10.1016/j.jelechem.2020.114723.
- Zhang, L., D. Huang, N. Hu, C. Yang, M. Li, H. Wei, Z. Yang, Y. Su, and Y. Zhang. 2017. Three-dimensional structures of graphene/polyaniline hybrid films constructed by steamed water for high-performance supercapacitors. *Journal of Power Sources* 342:1–8. doi:10.1016/j.jpowsour.2016.11.068.
- Zheng, L. H., M. H. Chen, S. X. Liang, and Q. F. Lü. 2021. Oxygen-rich hierarchical porous carbon derived from biomass waste-kapok flower for supercapacitor electrode. *Diamond and Related Materials* 113 (January):108267. doi:10.1016/j.diamond.2021.108267.

# Mission grass bio-waste functional carbon self-single-doped for ultrahigh energy symmetrical supercapacitor

## ORIGINALITY REPORT

12%

SIMILARITY INDEX

8%

INTERNET SOURCES

6%

PUBLICATIONS

6%

STUDENT PAPERS

## PRIMARY SOURCES

1	<a href="http://liu.diva-portal.org">liu.diva-portal.org</a> Internet Source	<1 %
2	<a href="http://report.ipcc.ch">report.ipcc.ch</a> Internet Source	<1 %
3	<a href="http://www.biofueljournal.com">www.biofueljournal.com</a> Internet Source	<1 %
4	<a href="http://2dc40e33-085f-40e0-8172-9a1f898c1942.filesusr.com">2dc40e33-085f-40e0-8172-9a1f898c1942.filesusr.com</a> Internet Source	<1 %
5	Submitted to Swinburne University of Technology Student Paper	<1 %
6	T. Navrátil, M. Kopanica. "Analytical Application of Silver Composite Electrode", Critical Reviews in Analytical Chemistry, 2002 Publication	<1 %
7	Submitted to Universiti Sains Islam Malaysia Student Paper	<1 %
8	Shujahadeen B. Aziz, M.H. Hamsan, M.A. Brza, M.F.Z. Kadir, S.K. Muzakir, Rebar T.	<1 %



Abdulwahid. "Effect of glycerol on EDLC characteristics of chitosan:methylcellulose polymer blend electrolytes", Journal of Materials Research and Technology, 2020

Publication

---

9	Submitted to Univerza v Ljubljani Student Paper	<1 %
10	ia804503.us.archive.org Internet Source	<1 %
11	Submitted to Signature School Student Paper	<1 %
12	acikerisim.ozal.edu.tr Internet Source	<1 %
13	wsiz.edu.pl Internet Source	<1 %
14	Submitted to Karunya University Student Paper	<1 %
15	Zhen Wang, Gary S. Dwyer, Drew S. Coleman, Avner Vengosh. "Lead Isotopes as a New Tracer for Detecting Coal Fly Ash in the Environment", Environmental Science & Technology Letters, 2019 Publication	<1 %
16	dro.deakin.edu.au Internet Source	<1 %
17	A.K.M. Mohsin, Syed Far Abid Hossain, Hasanuzzaman Tushar, Mohammed Masum Iqbal, Alamgir Hossain. "Differential game	<1 %

model and coordination model for green supply chain based on green technology research and development", Heliyon, 2021

Publication

18

Submitted to Indian School of Mines

Student Paper

<1 %

19

Submitted to Nanyang Technological University

Student Paper

<1 %

20

Shujuan Meng, Qiong Su, Ping Zhang, Wanhong Sun, Yanbin Wang. "Temperature controlled hydrothermal synthesis of  $\gamma$ -MnOOH, Mn<sub>3</sub>O<sub>4</sub> and MnCO<sub>3</sub> on carbon cloth for supercapacitor application", CrystEngComm, 2020

Publication

<1 %

21

[cy.iitr.ac.in](http://cy.iitr.ac.in)

Internet Source

<1 %

22

[eaapublishing.org](http://eaapublishing.org)

Internet Source

<1 %

23

Petra Hribovšek, Emily Olesin Denny, Håkon Dahle, Achim Mall et al. "Novel hydrogen- and iron-oxidizing sheath-producing Zetaproteobacteria thrive at the Fåvne deep-sea hydrothermal vent field", Cold Spring Harbor Laboratory, 2023

Publication

<1 %

24

Won-Ki Kim, Jeong-Min Kim, Kumar Vikrant, Ki-Hyun Kim. "Performance validation of a

<1 %

non-photocatalytic air purifier built by reactive adsorbent against a commercial UV-based air purifier", Chemical Engineering Journal, 2023

Publication

25

[jnep.sumdu.edu.ua](http://jnep.sumdu.edu.ua)

Internet Source

<1 %

26

[rcastoragev2.blob.core.windows.net](http://rcastoragev2.blob.core.windows.net)

Internet Source

<1 %

27

Qiang Sun, Bin He, Xiang-Qian Zhang, An-Hui Lu. "Engineering of Hollow Core-Shell Interlinked Carbon Spheres for Highly Stable Lithium-Sulfur Batteries", ACS Nano, 2015

Publication

<1 %

28

Roslinda Zulkifli, Mohamad Deraman, Rusli Daik, Maria Muhammad Ishak et al.

"Electrochemical Characterization of Supercapacitor Electrodes Prepared by Activation of Green Monoliths Consist of Self-Adhesive Carbon Grains and Lignin", Materials Science Forum, 2016

Publication

<1 %

29

Submitted to School of Business and Management ITB

Student Paper

<1 %

30

[jmmm.material.chula.ac.th](http://jmmm.material.chula.ac.th)

Internet Source

<1 %

31

[samafind.sama.gov.sa](http://samafind.sama.gov.sa)

Internet Source

<1 %

32	<a href="http://ar.booksc.eu">ar.booksc.eu</a> Internet Source	<1 %
33	<a href="http://hal.archives-ouvertes.fr">hal.archives-ouvertes.fr</a> Internet Source	<1 %
34	<a href="http://www.depot.ceon.pl">www.depot.ceon.pl</a> Internet Source	<1 %
35	<a href="http://encyclopedia.pub">encyclopedia.pub</a> Internet Source	<1 %
36	Wenchao Duan, César Fernández-Sánchez, Martí Gich. "Upcycling Bread Waste into a Ag-Doped Carbon Material Applied to the Detection of Halogenated Compounds in Waters", ACS Applied Materials & Interfaces, 2022 Publication	<1 %
37	<a href="http://bioresourcesbioprocessing.springeropen.com">bioresourcesbioprocessing.springeropen.com</a> Internet Source	<1 %
38	Ahmad Nazrul Rosli, Muhammad Mus'ab Anas, Halimatus Saadiah. "The Study of a Structural and Electronic Properties of Two-Dimensional Flat Layer Arsenene Using Planewaves Density Functional Calculation", Solid State Phenomena, 2020 Publication	<1 %
39	Submitted to Napier University Student Paper	<1 %
40	Submitted to South Bank University Student Paper	<1 %



- |    |   |      |
|----|---|------|
| 41 | <a href="http://beilstein-journals.org">beilstein-journals.org</a><br>Internet Source   | <1 % |
| 42 | <a href="http://aip.scitation.org">aip.scitation.org</a><br>Internet Source   | <1 % |
| 43 | Jing Di, Xincui Fu, Huajun Zheng, Yi Jia. "H-TiO <sub>2</sub> /C/MnO <sub>2</sub> nanocomposite materials for high-performance supercapacitors", Journal of Nanoparticle Research, 2015<br>Publication                            | <1 % |
| 44 | Lingqi Huang, Zhiyong Luo, Mingwu Luo, Qi Zhang, He Zhu, Kaiyuan Shi, Shiping Zhu. "One-step synthesis of nitrogen-fluorine dual-doped porous carbon for supercapacitors", Journal of Energy Storage, 2021<br>Publication         | <1 % |
| 45 | <a href="http://fjfsdata01prod.blob.core.windows.net">fjfsdata01prod.blob.core.windows.net</a><br>Internet Source   | <1 % |
| 46 | El-Nahass, M.M.. "Investigation of electrical conductivity in Schottky-barrier devices based on nickel phthalocyanine thin films", Journal of Alloys and Compounds, 20070314<br>Publication                                       | <1 % |
| 47 | Fen Zhou, Shumeng Guan, Yizhi Yan, Mu Pan. "Polyaniline-derived nitrogen- and oxygen-decorated hierarchical porous carbons as an efficient electrode material for supercapacitors", Journal of Solid State Electrochemistry, 2020 | <1 % |

48 S. Myung, M. Lee, G. T. Kim, J. S. Ha, S. Hong. "Large-Scale "Surface-Programmed Assembly" of Pristine Vanadium Oxide Nanowire-Based Devices", *Advanced Materials*, 2005  $<1\%$

Publication

---

49 Ting Xiao, Pengcheng Che, Shulin Wang, Wenjie Zhou et al. "A novel two-prong strategy to boost the capacitive performance of commercial carbon cloth", *Journal of Alloys and Compounds*, 2020  $<1\%$

Publication

---

50 Submitted to University of Bristol  $<1\%$

Student Paper

---

51 [elib.dlr.de](http://elib.dlr.de)  $<1\%$

Internet Source

---

52 [vmis.um.edu.my](http://vmis.um.edu.my)  $<1\%$

Internet Source

---

53 Yuru Ge, Xuan Xie, Jessica Roscher, Rudolf Holze, Qunting Qu. "How to measure and report the capacity of electrochemical double layers, supercapacitors, and their electrode materials", *Journal of Solid State Electrochemistry*, 2020  $<1\%$

Publication

---

Exclude quotes Off

Exclude matches Off

Exclude bibliography Off